



KEK Preprint 94-20  
May 1994  
H

94 344 C

$\Lambda$  hyperon production at backward angles in the reaction  
 $\pi^- {}^6\text{Li} \rightarrow \Lambda X$  at 4 GeV/c

K. Tomizawa<sup>1</sup>, I. Arai, H. Kitayama<sup>1</sup>, N. Kato<sup>2</sup>, Y. Nagasaka<sup>3</sup>, M. Tanaka<sup>3</sup>, K. Yagi  
*Institute of Physics, University of Tsukuba, Tsukuba, Ibaraki 305, Japan*

J. Chiba, T. Kobayashi<sup>4</sup>, A. Manabe  
*National Laboratory for High Energy Physics, Tsukuba, Ibaraki 305, Japan*

T. Nagae, M. Sekimoto  
*Institute for Nuclear Study, University of Tokyo, Tanashi, Tokyo 188, Japan*  
and

V. Partuev  
*Institute for Nuclear Research, Moscow 117 312, Russia*

Abstract

The first measurement of the invariant cross sections and polarizations of  $\Lambda$  hyperons produced by the reaction  $\pi^- {}^6\text{Li} \rightarrow \Lambda X$  at 4 GeV/c in the backward angular region ( $70^\circ < \theta_{lab} < 145^\circ$ ) has been done. In the measured region the production with free nucleons was kinematically forbidden. All the experimental results are reproduced by a quark-parton model calculation.

*Submitted to Phys. Lett. B.*

SCAN-9409291



CERN LIBRARIES, GENEVA

**National Laboratory for High Energy Physics, 1994**

KEK Reports are available from:

Technical Information & Library  
National Laboratory for High Energy Physics  
1-1 Oho, Tsukuba-shi  
Ibaraki-ken, 305  
JAPAN

Phone: 0298-64-1171  
Telex: 3652-534 (Domestic)  
(0)3652-534 (International)  
Fax: 0298-64-4604  
Cable: KEK OHO  
E-mail: LIBRARY@JPNKEK.VX (Bitnet Address)  
library@kek.vax.kek.jp (Internet Address)

The particle production in the backward-angular region, in which the particle production by the reaction of an incident hadron with a free nucleon is kinematically forbidden, has been expected to provide crucial information for the study of many-body effects in the nucleus because of its exotic kinematics. Many experiments were studied this region, measuring the invariant cross section by using a variety of incident particles, e.g.,  $\pi$ ,  $p$ ,  $d$ ,  $e$  and  $\mu$ , and detecting a variety of emitted particles, e.g.,  $\pi$ ,  $p$ ,  $K$ ,  $\Lambda$  and  $d$  [1]. These measurements were mostly restricted to fixed angles, and only a few bubble chamber measurements cover a wide angular range.

The measurement of  $\Lambda$  hyperon production has several unique characteristics. First, a strange(*s*)-quark does not exist in usual nuclear matter, so that the production of a  $\Lambda$  hyperon means the production of an  $\bar{s}$ -*s* quark pair from nuclear matter, followed by their recombination with the other quarks. In this context, the  $\Lambda$  hyperon works as a fascinating nuclear probe on the quark level. Secondly, the strong interaction between a nucleon and a  $\Lambda$  hyperon is weaker than that between two nucleons, e.g., the strength of nucleon- $\Lambda$  interaction is two thirds the strength of the nucleon-nucleon interaction, in a model with combined quark-gluon exchange [2]. This reaction may be free from complicated final-state interactions as compared with backward nucleon production. Thirdly, the  $\Lambda$  hyperon decays into  $p$  and  $\pi^-$  via the weak interaction with a branching ratio of 64.2%. Since the weak interaction does not conserve parity, the angular distribution in the center of mass system shows an asymmetry depending on the polarization of the  $\Lambda$  hyperon. Because of this asymmetry, we can measure the  $\Lambda$  hyperon's polarization easily and efficiently through observing the pattern of its  $p, \pi^-$  decay. The polarization is thought to be an observable sensitive to the underlying reaction mechanism.

In the past, we have carried out an experiment of backward  $\Lambda$  production;  $\pi^- {}^{12}\text{C} \rightarrow \Lambda X$  at 4 GeV/c [3]. As the next step, we have proceeded to study the nuclear mass-number dependence of the reaction, i.e.,  $\pi^- {}^6\text{Li} \rightarrow \Lambda X$  at 4 GeV/c. The experimental setup is shown in fig.1. The detector system used in the experiment was a combination

of a cylindrical detector system (CDS) of FANCY [4] with a dedicated vertex detection system, i.e., target chambers (TC's: TC1 to TC4) and a vertex chamber (VC). It was placed at the  $\pi^2$  beam line of the 12 GeV proton synchrotron (12 GeV PS) in the National Laboratory for High Energy Physics in Japan (KEK). The beam particles were defined by a five-fold coincidence of four plastic scintillation counters (S0 to S3) and a threshold type gas cherenkov counter (GC). The beam chambers (BC's: BC1 to BC4) and TC's [5], which are multi-wire proportional chambers, measured the position of beam particles on the target. The CDS of FANCY consists of three parts, i.e., a solenoidal magnet with an operating field of 3 kG, a cylindrical drift chamber (CDC) and a cylindrical hodoscope (CDH). The CDC is a jet-chamber type of cylindrical drift chamber for measuring the momentum and trajectory of the outgoing particles with a momentum resolution of  $\Delta P/P \sim 10\%$ . The CDH consists of 24 plastic scintillation counters, and surrounds the CDC. These counters were used to measure the time-of-flight of the outgoing particles. The VC is a cylindrical drift chamber, which was placed in the CDC, and was used to detect a vertex point by measuring the trajectories of the  $\Lambda$  hyperon's decay products  $p$  and  $\pi^-$ . An enriched nuclear target of  ${}^6\text{Li}$  (93%), which was 36 mm thick and 32 mm in diameter, was placed in the inner open space of the VC.

The  $\Lambda$  hyperon was identified by observing its decay of  $\Lambda \rightarrow p \pi^-$ . To select  $\Lambda$  production events, we adopted the following criteria: (I) The distance between the reaction point on the target and the decay vertex point was greater than 5 mm. (II) The angular difference between the vector from the reaction point to the decay vertex point and the momentum vector of the  $\Lambda$  hyperon was within 40 degrees. (III) The angular difference between the momentum vectors of the  $p$  and the  $\pi^-$  was greater than 30 degrees and less than 150 degrees. The resulting invariant-mass spectrum of the  $\Lambda$  hyperons under the selection criteria (I)-(III) is shown in fig.2.

The invariant cross sections in terms of kinetic energy  $T$  and emission angle  $\theta$  in

the laboratory system are calculated by the following equation;

$$\frac{1}{P} \frac{d\sigma(\theta, T)}{dT d\Omega} = \frac{1}{P} \frac{N(\theta, T)}{\eta \cdot \epsilon \cdot \tau_{decay}} \cdot \frac{1}{\Delta T \cdot \Delta\Omega \cdot I \cdot N_t} ,$$

where  $P$  is the momentum of  $\Lambda$  hyperon in the laboratory system,  $\Omega$  is the solid angle,  $I$  and  $N_t$  are number of beam particles passing through the target and number of nuclei in the target per unit area, respectively. The number of  $\Lambda$  hyperons  $N(\theta, T)$ , which was given in  $\Delta T \cdot \Delta\Omega$  region, was estimated by fitting each mass spectrum using the following model function;

$$\frac{\lambda_1}{\sqrt{2\pi}\lambda_2} \exp\left(-\frac{(x - \lambda_3)^2}{2\lambda_2^2}\right) + \lambda_4 f(x) ,$$

where  $x$  is an invariant mass, the first term represents the  $\Lambda$  mass spectrum with a certain mass resolution of detector and  $f(x)$  is the background (BG) mass spectrum. The  $f(x)$  is fixed by using a spline function obtained by fitting the 'other side' background (OSBG), in which we took  $p\pi^-$  pairs under the same selection criteria described above but with the angular difference defined in (II) larger than 140 degrees, i.e. the other side of normal selection. Because both BG and OSBG are given under the same geometrical condition, they should be the same distribution. The values of parameters  $\lambda$ 's were determined by the least-squares method. As expected,  $\lambda_4 = 1.00 \pm 0.01$  was obtained, typically. We have defined the  $\lambda_1$  as  $N(\theta, T)$ .  $\epsilon$  is the efficiency of detector system,  $\eta$  is the acceptance correction factor including the selection efficiency by the above selection criteria (I)–(III), which is calculated by using a Monte Carlo method, and  $\tau_{decay}$  is a decay branching ratio of  $\Lambda \rightarrow p\pi^-$ . The systematic error for the absolute cross section was evaluated by considering change of parameters used in the above reduction, and was  $\pm 18\%$  typically.

We have measured the invariant cross sections shown in fig.3a. In order to understand the measured results, we have carried out a calculation based on a quark-parton model of nuclear production [6], which works well over a wide incident energy region from 6 GeV to 400 GeV, and a Thomas precession model of hyperon polarization [7].

In these models, the following assumptions were made. (I) A  $\Lambda$  hyperon is produced through recombination of a spin-singlet diquark  $(ud)_0$  and a strange quark ( $s$ ) in nuclear fragmentation where the absorption of the diquark is taken into account and the rescattering of it is not. (II) The dynamical origin of  $\Lambda$  polarizations arises from the Thomas precession of the  $s$ -quark's spin in the recombination process. (III) When the incident  $\pi$  collides with the target nucleus, it interacts with the nucleons that lie within an imaginary tube of cross section  $\sigma_i(\pi p) = 26 \text{ mb} = \pi(0.9 \text{ fm})^2$  drawn along its straight path through the nucleus. (IV) For simplicity, the secondary processes; e.g.,  $\Sigma N$  conversions and  $\pi K$  reactions, were not considered and the possible final state interaction between the  $\Lambda$  hyperon and the residual nucleus was not considered either.

The invariant cross section was calculated by the following expressions;

$$\begin{aligned} E \frac{d\sigma}{d\vec{P}} &= \sum_{i=1}^6 \frac{E^*(i)}{P_{max}^*(i)} \frac{d^2\sigma(i)}{dx_{Di}(i) d\vec{P}_T} , \\ d^2\sigma(i) &= \sigma(\pi^- {}^6\text{Li}) C_{\Lambda}^D(i) P(i; 6) \left[ (1/3) \gamma_D(i) D_i(x_{Di}) + (2/3) \gamma_D(i) D_i^1(x_{Di}) \right] \\ &\quad \cdot f(\vec{P}_T) dx_{Di}(i) d\vec{P}_T , \\ f(\vec{P}_T) &= \frac{1}{2\pi \cdot 1.45} \left[ 10 \exp(-10 P_T^2) + 0.45 \cdot 2.7 \exp(-2.7 P_T^2) \right] , \quad P_T \text{ in GeV}/c , \end{aligned}$$

where  $E^*(i)$  and  $P_{max}^*(i)$  are the energy and the maximum available momentum of the  $\Lambda$  in the c.m. system of the  $\pi^-$  and the  $i$ -nucleon tube respectively,  $x_{Di}$  is the Feynman scaling variable  $P_L^*(i)/P_{max}^*(i)$  in which  $P_L^*(i)$  is the longitudinal momentum of  $\Lambda$  hyperon in the c.m. system of  $\pi^-$  and  $i$ -nucleon tube,  $\gamma_D(i)$  is an attenuation factor of the diquark in the  $i$ -nucleon tube and  $f(\vec{P}_T)$  is a universal  $\vec{P}_T$  distribution of valence quarks obtained from  $pp$  collisions [6]. The total cross section  $\sigma(\pi^- {}^6\text{Li})$  is given as 123 mb. This value is evaluated by extrapolation of the total inelastic cross sections on various targets [8].  $D_i(x_{Di})$  ( $D_i^1(x_{Di})$ ) and  $P(i; 6)$  are the diquark (wounded diquark)  $(ud)_0$  distribution function and the probability of finding the  $i$ -nucleon tube in the target nucleus  ${}^6\text{Li}$ , respectively.  $C_{\Lambda}^D(i)$  is a recombination factor for the diquark to recombine with an  $s$ -quark from the sea to form a  $\Lambda$  hyperon in the  $i$ -nucleon tube.

In the present calculation, we assumed  $C_{\Lambda}^D(i) = 0.04i$  considering its possible dependence on the number of nucleons in the tube, while  $C_{\Lambda}^D(1) = 0.04$  [6] was obtained by fitting the experimental data on  $pA \rightarrow \Lambda(0^\circ)$  at 300 GeV, where  $A = \text{Be, Cu and Pb}$ , which is considered to be a proton fragmentation on the nucleus. This dependence of  $C_{\Lambda}^D$  on the number of participant nucleons is not trivial. Indeed, the  $K^+/\pi^+$  ratio measured at backward angles [9] seems to suggest significant enhancement of  $C_{\Lambda}^D$  in the region of  $x_F > 1$ , where more than one nucleon participates. This behavior may be considered to be related to nontrivial quark-gluon structure of nucleus. If an effective confinement size is changed by the clustering of  $i$ -nucleons, enhanced sea quarks will be produced according to ref.10. The enhancement is proportional to the number of nucleons  $i$  for small  $x$  under simplified calculation. Moreover, the effect of the chemical potential of nuclear matter will suppress the enhancement of non-strange sea. As a result, the strange sea may be enhanced relative to the nonstrange sea. The calculation (solid curves) has reproduced the measured cross sections very well. In addition, the calculation for  $^{12}\text{C}$  target is shown in fig.3b together with our previous measurement [3]. The calculation has also reproduced the data quite well. It should be noted that the quark parton model for the backward  $\Lambda$  production by taking  $C_{\Lambda}^D = 0.04$ , which is presumably suggested by the calculation for the backward pion production [6], can predict only about half of the measured cross sections.

Fig.4 shows the dependence of differential cross sections integrated over the range of kinetic energies from 50 to 160 MeV on the target mass number  $A$  in the reaction  $\pi^- A \rightarrow \Lambda(90^\circ)X$  at 5 GeV/c [11]. Our results on both  $^6\text{Li}$  and  $^{12}\text{C}$ -targets at 4 GeV/c, are also shown in fig.5. The quark-parton model calculations for the case of  $C_{\Lambda}^D(i) = 0.04i$  and  $C_{\Lambda}^D = 0.04$  have been done for these data. The calculation with  $C_{\Lambda}^D(i) = 0.04i$  (solid curve) reproduces the data very well over the wide range of nuclear mass number from  $^6\text{Li}$  to  $^{208}\text{Pb}$ , while that with  $C_{\Lambda}^D = 0.04$  does not especially for heavier nuclei.

We have also measured the polarization of  $\Lambda$  hyperons as shown in fig.5. The

perpendicular  $\vec{n}$  to the production plane corresponds to the axis of the  $\Lambda$  polarization. We define the positive polarization as a direction of  $\vec{n} = \vec{P}_{beam} \times \vec{P}_{\Lambda}$ , i.e., the Basel convention, where  $\vec{P}_{beam}$  and  $\vec{P}_{\Lambda}$  are the momentum vectors of the incident beam particle and the  $\Lambda$  hyperon, respectively. The systematic asymmetry was checked by using of the "polarization" asymmetry of  $K_S^0$  particles, which should be zero because it has a spin 0. The procedure of the reduction of polarizations is the same as that in ref.3. The asymmetry of  $K_S^0$  was obtained as  $-0.04 \pm 0.08$ . This value of systematic bias is negligible in our result. A quark-parton model calculation is also shown. It seems consistent with our measurement.

In conclusion, we have measured the invariant differential cross sections and polarizations of  $\Lambda$  hyperons produced in the backward angular region ( $70^\circ < \theta_{lab} < 145^\circ$ ) in the reaction  $\pi^- ^6\text{Li} \rightarrow \Lambda X$  at 4 GeV/c. The  $\Lambda$  hyperon production in this region is kinematically forbidden in the reaction of  $\pi^-$  with a free nucleon. This is the first experimental measurement of backward  $\Lambda$  hyperon production on  $^6\text{Li}$  target. A calculation based on a quark-parton model has reproduced the measured cross sections very well under the ad hoc assumption for the behavior of the recombination factor  $C_{\Lambda}^D(i)$  between the  $(ud)_0$  diquark and the  $s$ -quark concerned, which is proportional to the number of participant nucleons  $i$ . Such behavior of  $C_{\Lambda}^D(i)$  may be considered to be related to the nontrivial quark-gluon structure of the nucleus, probably due to the clustering of nucleons. The target-mass number dependence of the cross section at  $90^\circ$  has been also reproduced very well over the wide range of mass number from  $^6\text{Li}$  to  $^{208}\text{Pb}$ . We have also measured the polarizations of  $\Lambda$  hyperons. It is consistent with the quark-parton model calculation.

We acknowledge all the staff of the KEK for their support of the present work. One of the authors (K. Tomizawa) would like to thank Professor T. Kohmura, Professor K. Kondo and Professor Y. Tagishi for their encouragement and valuable advice.

1. A.M. Baldin et al., Sov. J. Nucl. Phys. 18 (1974) 41;  
A.M. Baldin et al., Sov. J. Nucl. Phys. 20 (1975) 629;  
S. Frankel et al., Phys. Rev. Lett. 36 (1976) 642;  
J.P. Berge et al., Phys. Rev. D 18 (1978) 1376;  
L.S. Schroeder et al., Phys. Rev. Lett. 43 (1979) 1784;  
Y.D. Bayukov et al., Phys. Rev. C 20 (1979) 764;  
Y.D. Bayukov et al., Phys. Lett. B 85 (1979) 315;  
N.A. Nikiforov et al., Phys. Rev. C 22 (1980) 700.
2. H.J. Pirner, Phys. Lett. B 85 (1979) 190.
3. A. Manabe et al., Phys. Rev. Lett. 63 (1989) 490.
4. K. Ichimaru et al., Nucl. Instrum. Methods A 237 (1985) 559.
5. M. Ninomiya et al., Nucl. Instrum. Methods A 272 (1988) 727.
6. G. Berlad et al., Phys. Rev. D 22 (1980) 1547.
7. T.A. DeGrand and H.I. Miettinen, Phys. Rev. D 24 (1981) 2419.
8. B.M. Bobchenko et al., Sov. J. Nucl. Phys. 53 (1991) 458.
9. S.V. Boyarinov et al., Sov. J. Nucl. Phys. 50 (1989) 996.
10. J. Dias de Deus et al., Phys. Rev. D 30 (1984) 697.
11. L.S. Vorob'ev et al., ITEP 86-98 (1986);  
L.S. Vorob'ev et al., ITEP 87-126 (1987);  
L.S. Vorob'ev et al., Sov. J. Nucl. Phys. 53 (1991) 458.

- Fig.1. The set-up of the experiment. The spectrometer consists of beam-line detectors, a cylindrical spectrometer and a vertex detection system.
- Fig.2. The invariant-mass spectra of a  $p, \pi^-$  pair of under the selection criteria of (I)–(III). Solid curves are fitted results by the least-squares method.
- Fig.3. The invariant cross sections for the production of backward  $\Lambda$  hyperons versus its kinetic energy at each emission angle for (a)  ${}^6\text{Li}$ -target and (b)  ${}^{12}\text{C}$ -target [3]. The solid (dashed) curves are calculations based on the quark-parton model using  $C_\Lambda^D = 0.04i$  ( $C_\Lambda^D = 0.04$ ) for  ${}^6\text{Li}$  and  ${}^{12}\text{C}$ , respectively.
- Fig.4. The differential cross sections for  $\pi^-A \rightarrow \Lambda X$  at the  $90^\circ$  in the laboratory system integrated over the range of kinetic energies from 50 to 160 MeV, versus the target-mass number  $A$ . The open circles and diamonds are the data at 4 GeV/c and 5 GeV/c [11], respectively. The solid (dashed) curve is a calculation based on the quark-parton model with  $C_\Lambda^D(i) = 0.04i$  ( $C_\Lambda^D = 0.04$ ).
- Fig.5. The polarizations versus emission angles for the  ${}^6\text{Li}$  target. The solid curve is a calculation based on the quark-parton model.

FOOTNOTES

<sup>1</sup>Present address: ULVAC Japan Ltd., Chigasaki, Kanagawa 253, Japan

<sup>2</sup>Present address: Information & Communication System Laboratory, Toshiba Corporation, Kawasaki, Kanagawa 210, Japan

<sup>3</sup>Present address: National Laboratory for High Energy Physics, Tsukuba, Ibaraki 305, Japan

<sup>4</sup>Present address: The Institute of Physical and Chemical Research, Wako, Saitama 351-01, Japan

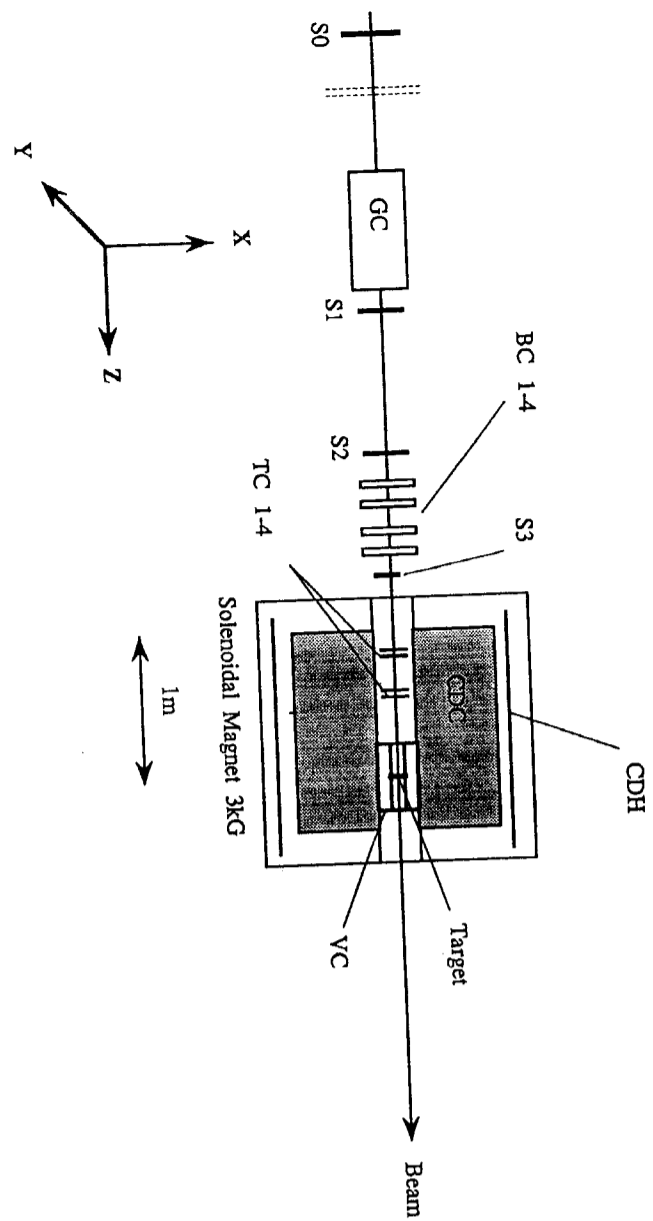


Fig. 1

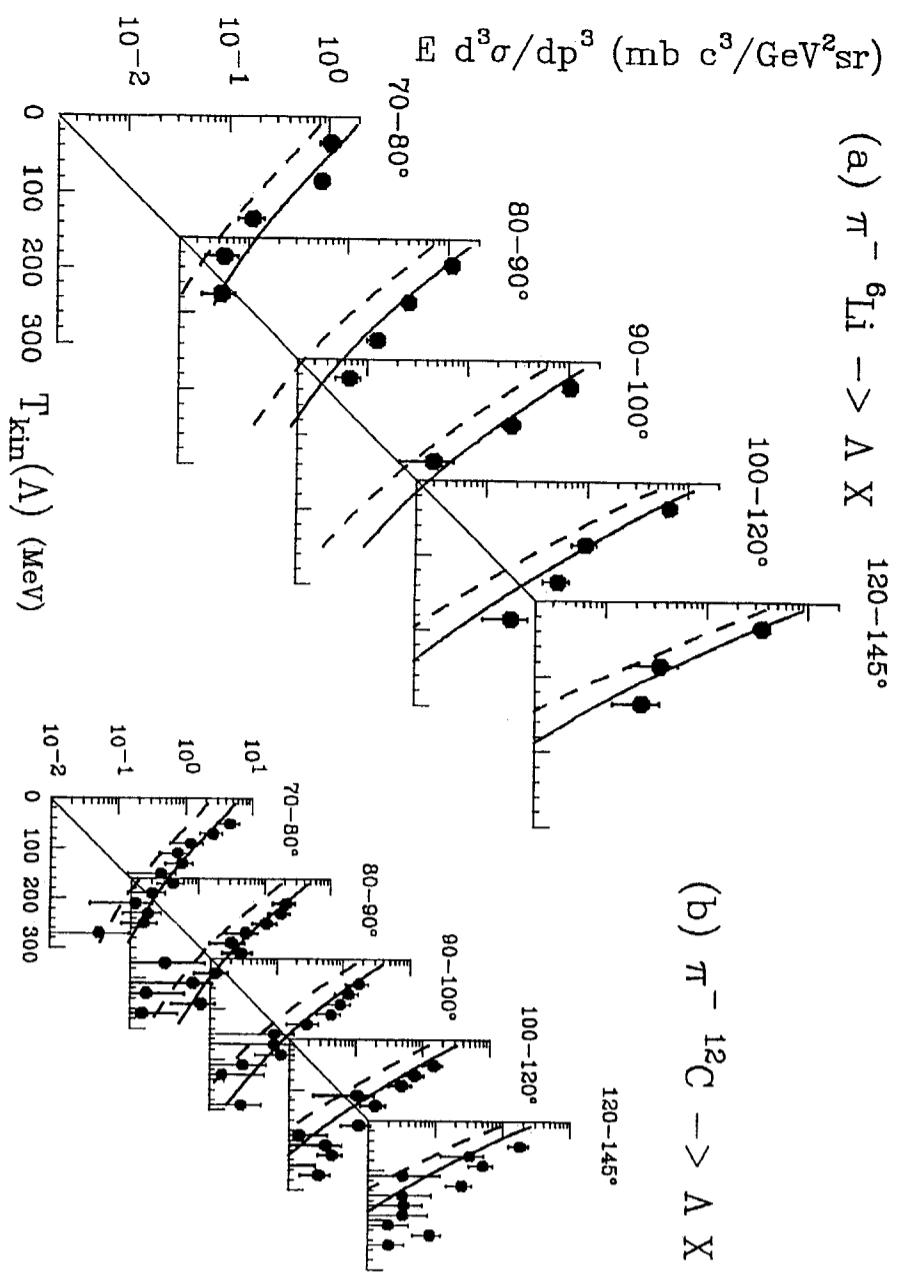


Fig. 3

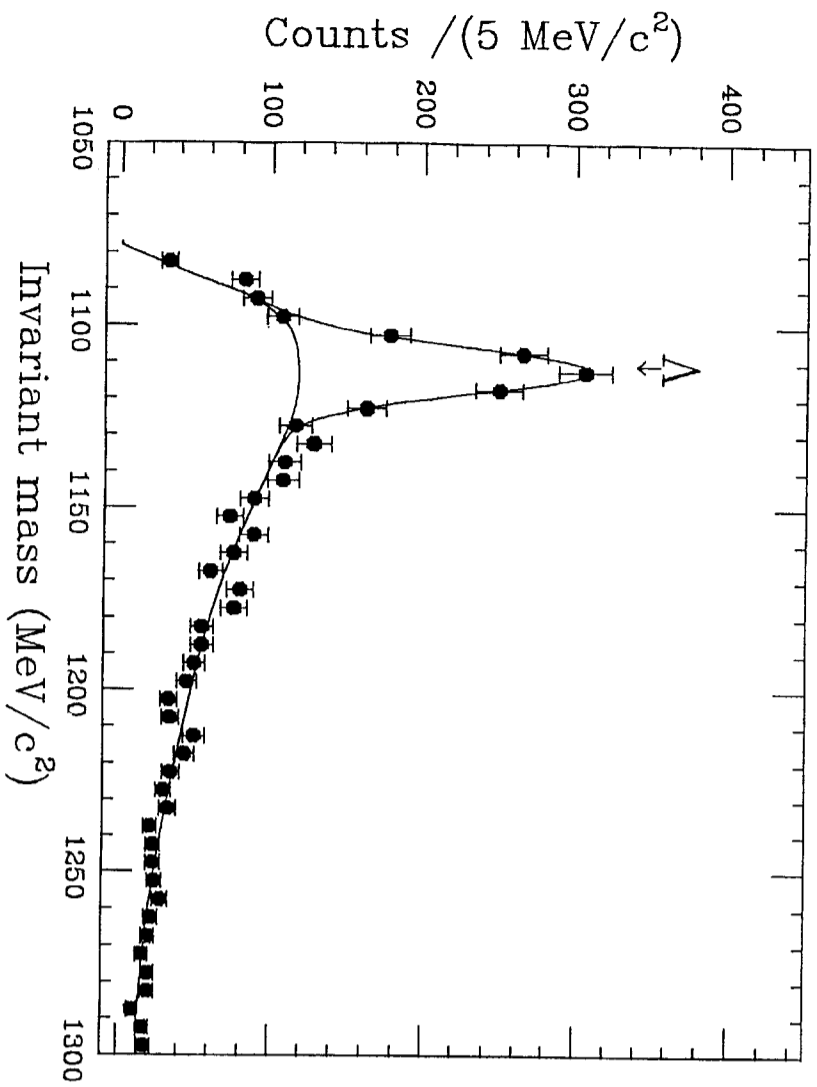


Fig. 2



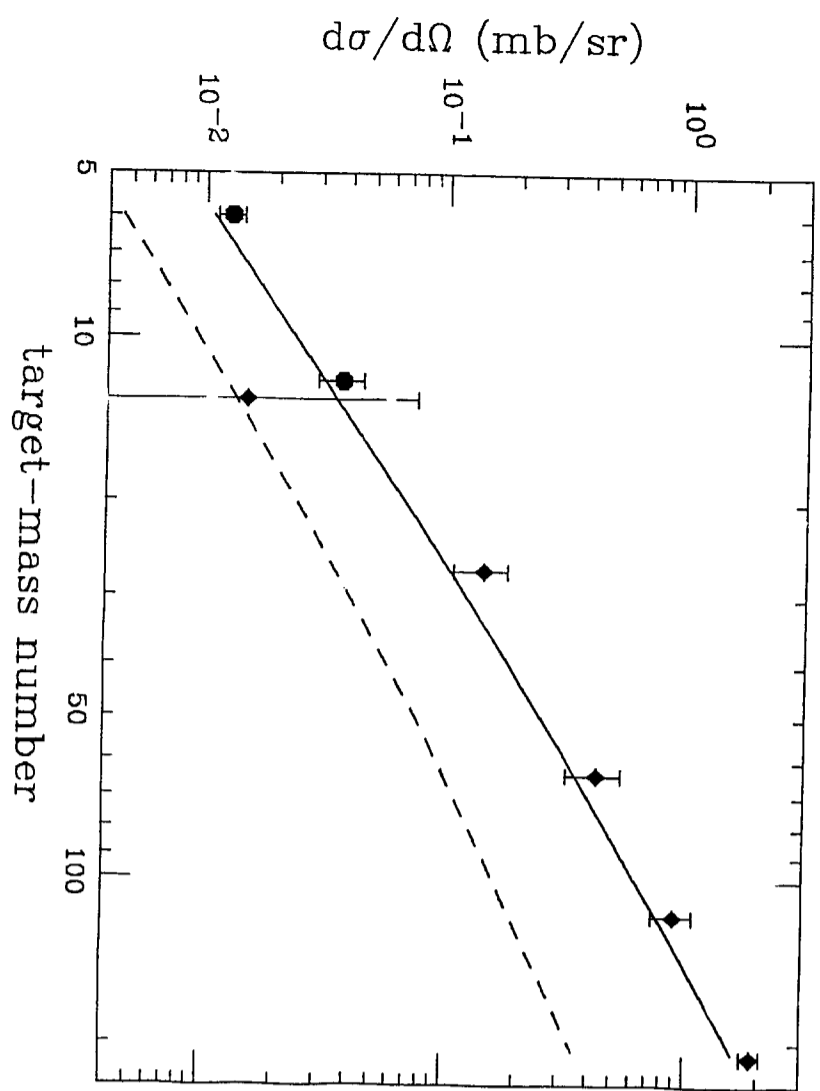


Fig. 4

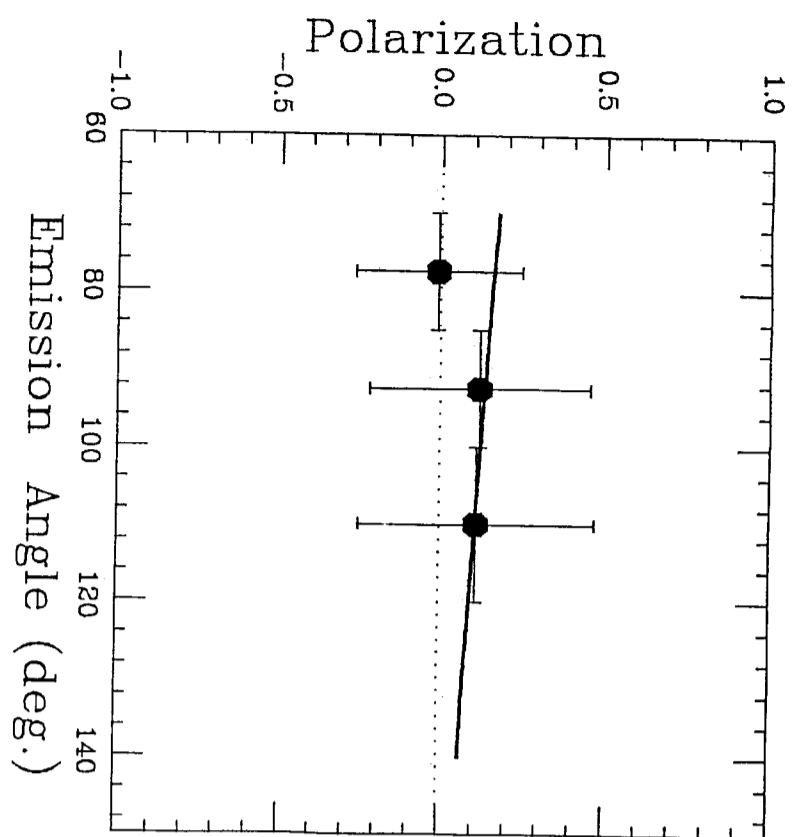


Fig. 5

